J Bioenerg Biomembr (2011) 43:531–539
DOI 10.1007/s10863-011-9374-3

Neuronal differentiation involves a shift from glucose oxidation to fermentation

Maynara Fornazari · Isis C. Nascimento · Arthur A. Nery · Camille C. Caldeira da Silva · Alicia J. Kowaltowski · Henning Ulrich

Received: 18 April 2011 / Accepted: 20 June 2011 / Published online: 21 July 2011

Abstract Energy metabolism in the adult brain consumes large quantities of glucose, but little is known to date regarding how glucose metabolism changes during neuronal differentiation, a process that is highly demanding energetically. We studied changes in glucose metabolism during neuronal differentiation of P19 mouse embryonal carcinoma cells, E14Tg2A embryonic stem cells as well as during brain development of BLC57 mice. In all these models, we find that neurogenesis is accompanied by a shift from oxidative to fermentative glucose metabolism. This shift is accompanied by both a decrease in mitochondrial enzymatic activities and mitochondrial uncoupling. In keeping with this finding, we also observe that differentiation does not require oxidative metabolism, as indicated by experiments demonstrating that the process is preserved in cells treated with the ATP synthase inhibitor oligomycin. Overall, we provide evidence that neuronal differentiation involves a shift from oxidative to fermentative metabolism, and that oxidative phosphorylation is not essential for this process.

Keywords Neuronal differentiation · Fermentative glucose metabolism · Mitochondrial uncoupling · P19 embryonal carcinoma cells · E14Tg2A embryonic stem cells

Electronic supplementary material The online version of this article (doi:10.1007/s10863-011-9374-3) contains supplementary material, which is available to authorized users.

M. Fornazari · A. A. Nery · C. C. Caldeira da Silva · A. J. Kowaltowski (✉) · H. Ulrich (✉)
Departamento de Bioquímica, Instituto de Química, Universidade de São Paulo, Av. Prof. Lineu Prestes, 748, 05508-900 São Paulo, SP, Brazil
e-mail: alicia@iq.usp.br
e-mail: henning@iq.usp.br

I. C. Nascimento
Departmento de Neurologia/Neurocirurgia, Universidade Federal de São Paulo, São Paulo 04023-900, Brazil

Introduction

The brain consumes large quantities of oxygen and glucose, which have long been assumed to be used to maintain neuronal activity (Bolaños et al. 2004). Indeed, neurons contain a large number of mitochondria, suggesting active oxidative phosphorylation, and exhibit a limited ability to metabolize substrates other than glucose (Cox and Bachelard 1982). However, despite the suggestion of the importance of oxidative phosphorylation in neurons, in vitro studies demonstrate that oxidative phosphorylation is not required for neuronal survival, as indicated by the ability to survive in culture in the presence of mitochondrial respiratory inhibitors rotenone and oligomycin (Budd and Nicholls 1996; Nicholls and Budd 1998; Castilho et al. 1998). Additionally, the conventional view that glucose oxidation is a hallmark of neuron metabolism must be questioned due to the evidence of an astrocyte-neuron lactate shuttle. Experimental evidence indicates that, during neuronal activity, energy requirements of the glia are met through glycolysis, while the released lactate is used as an energy source by neurons (Bittar et al. 1996; Magistretti 2006; Pellerin and Magistretti 1994; Sibson et al. 1998; Hyder et al. 2006; Tsacopoulos and Magistretti 1996; Véga et al. 1998).

Furthermore, some publications suggest that neurons contribute minimally to glucose consumption in the brain (Kasischke et al. 2004; Pauwels et al. 1985), although others have indicated that both neurons and glia have high rates of glucose utilization and oxidative metabolism (Hertz 2007). Indeed, in brain slices, pyruvate and lactate can be metabolized and support the production of high-energy phosphates, but are not enough to maintain neural activity (Mcllwain and Bachelard 1985; Yamane et al. 2000; Wada et al. 1998). Okada and coworkers reported that anaerobic glycolysis is crucial for neural activity and that lactate cannot preserve neural activity in the physiological state (Yamane et al. 2000). While the participation of different energy metabolism pathways in neurons is controversial, even less is known about changes occurring during neuronal differentiation, although the process is accepted to involve large energy requirements which would be most effectively provided by oxidative phosphorylation (Bernstein and Bamburg 2003). In general, undifferentiated cells are believed to present a predominance of fermentative glycolysis over oxidative phosphorylation (Warburg 1956; Rehman 2010). However, most studies on this topic involve cancer cells or laboratory cell lines cultured and selected under high glucose conditions, which may present very different metabolic characteristics relative to neuronal precursor cells.

Cellular differentiation can be studied in vitro using model systems that closely resemble development in vivo. Mouse embryonic (ES) and carcinoma (EC) stem cell lines can be maintained and replicated, keeping their pluripotency. These cell lines can also be induced to differentiate into cell types originating from the three germ layers (Soprano et al. 2007). The murine EC P19 cell line, which displays characteristics of ES cells from blastocysts, has been used for decades to study mechanisms of differentiation (Keller 2005). This pluripotent cell line was obtained from a C3H/HE teratocarcinoma (Bain et al. 1995; Jones-Villeneuve et al. 1982), and, in response to retinoic acid (RA), forms embryoid bodies and differentiates into neurons and glia (Ulrich and Majumder 2006). The E14Tg2A line, originally derived from 129 strain/Ola mouse blastocysts (Hooper et al. 1987), is cultured in the absence of a feeder layer and can be maintained in an undifferentiated state in the presence of Leukemia Inhibitory Factor (LIF). When LIF is removed, E14Tg2A cells differentiate into a variety of cell types, both spontaneously and via inductive agents as retinoic acid (Bain et al. 1994; Dinsmore 1996; Fraichard et al. 1995).

Here, we study changes in glucose metabolism during neuronal differentiation in vitro, using P19 and E14Tg2A cells, and in vivo, using mouse brains at different developmental stages. Our work provides solid evidence that glucose fermentation becomes more prevalent during neuronal differentiation, while oxidative phosphorylation is unnecessary for this process.

Experimental procedures

Materials

Reagents used were of the highest purity available and, if not otherwise stated, purchased from Sigma-Aldrich Chemicals. All aqueous solutions were prepared in deionized, double-distilled water. Retinoic acid (RA), CCCP and oligomycin were dissolved in DMSO, and oxaloacetate was prepared in water. DTNB and oxaloacetate were prepared just prior to each experiment.

Culture and differentiation of P19 cells

P19 mouse embryonal carcinoma cells were cultured in High Glucose DMEM buffered with 10 mM HEPES, pH 7.4, containing 10% fetal bovine serum (FBS) and 2 mM sodium pyruvate. P19 cell cultures were kept subconfluent in order to avoid medium acidification and spontaneous induction of differentiation, at 37 °C, in a water saturated atmosphere containing 5% CO2. For induction of neuronal differentiation, 10^7 P19 cells were transferred into 20 mL of defined, serum-free medium composed of High Glucose DMEM, buffered with 10 mM HEPES pH 7.4 and containing 2 mM sodium pyruvate, 5 mg/mL bovine pancreas insulin, 30 mg/mL human apo-transferrin, 20 μM ethanolamine and 30 nM sodium selenite in the presence of 1 mM all-trans-retinoic acid in 125 mm size non-adherent plates (Resende et al. 2007, 2008a,b). Embryoid bodies were then collected from the floating culture, transferred into 270 mL cell culture flasks and kept in serum containing media for 48 h. Cells were kept in defined media from the fourth day on. On the fifth day of differentiation, 5 μg/ml cytosine arabinoside was added to eliminate proliferating glial cells, except where noted in the text. Neuronal differentiation was completed around day 8, as judged by peak expression levels of the neuron-specific protein βIII tubulin. For the investigation of the effects of oxidative phosphorylation on neuronal differentiation, cells were cultured from day 0 on with 1 μg/mL oligomycin. Oligomycin was readministered with medium changes, performed every 48 h. Control cells were treated with equal quantities of DMSO, the solvent of oligomycin.

Culture and differentiation of E14Tg2A mouse embryonic stem cells

The feeder-cell independent E14Tg2A embryonic stem (ES) cell line was kindly provided by Dr. Deborah Schechtman, *Instituto de Química, Universidade de São Paulo*. Cells were cultured in DMEM containing 15% Fetal Bovine Serum (FBS), 2 mM sodium pyruvate, 1% non essential amino acids, 10^3 U/mL Leukemia Inhibitory

Factor (LIF), 0.1 mM β-mercaptoethanol and 10 mM HEPES, pH 7.4, at 37 °C in a water-saturated atmosphere containing 5% CO_2. For neuronal differentiation, 5.10^6 cells were cultured in 90×15 mm nonadherent plates in DMEM supplemented with 20% FBS, 1% non-essential amino acids and 0.1 mM β-mercaptoethanol for 48 h to induce embryoid body formation. Following substitution of the culture medium, cells were cultured as a suspension for 4 further days in the presence of 2 mM RA. Embryoid bodies were plated in 125 mm adherent cell culture flasks and cultured 4 days further in order to complete neural differentiation.

Immunocytochemistry

For immunocytochemical detection of marker proteins specific for respective differentiation stages, P19 and E14Tg2A cells were grown and induced to differentiate in 24 well plates. Cells were fixed with 4% paraformaldehyde in phosphate-buffered saline (PBS) for 15 min, washed three times with PBS and then incubated for 30 min in a blocking solution containing 0.05% Triton-X 100 and 2% FBS. Cells were incubated overnight at 4 °C with polyclonal primary antibodies raised against mouse monoclonal anti stage-specific embryonic antigen-1 (SSEA-1) (1:200, Chemicon) or anti-βIII tubulin antibodies (1:200, Millipore). The slides were washed three times with PBS, followed by two hour incubation with Cy3-conjugated goat anti-mouse (1:800, Sigma). In control experiments, the primary antibody was omitted, and immunostaining was never observed. Counterstaining of cell nuclei was achieved with 0.1% of 4′,6-diamidino-2-phenylindole (DAPI). After washing with PBS, the slides were mounted with Vectashield (Vector Laboratories, Burlingame, CA) and examined on an Axiovert 200 epifluorescence microscope (Zeiss), equipped with a Nikon DMX1200F camera and Metamorph image analysis program.

Western blotting assays

Undifferentiated and differentiated P19 cells (day 8) were homogenized and then used for membrane-protein preparation by differential centrifugation as described elsewhere (Resende et al. 2008a). Forty micrograms of membrane protein were run on a SDS-polyacrylamide gel and electroblotted onto Polyvinylidene fluoride (PVDF) membranes. The incubation with primary and secondary antibodies was carried out as already described by Resende et al. 2008a. Primary antibodies used were anti-βIII tubulin (Millipore, 1:5,000) and anti-β actin (Sigma, 1:5,000). Horse radish peroxidase-conjugated goat anti mouse (Jackson, 1:5,000) was employed for visualization of immunostaining.

Calcium imaging

Undifferentiated and neuronal-differentiated P19 and E14Tg2A cells were loaded with 5 μM Fluo3-AM and used in calcium-imaging experiments. Cells were maintained in extracellular medium containing 140 mM NaCl, 3 mM KCl, 2.5 mM $CaCl_2$, 10 mM glucose and 10 mM HEPES, pH 7.4. Stimulation by neurotransmitters was performed at 1 mM of each agonist. A Ca^{2+} ionophore (ionomycin; 5 μM) was added to the cells followed by EGTA (10 mM) to determine maximal (Fmax) and minimal (Fmin) fluorescence values, respectively. $[Ca^{2+}]_i$ values were calculated from Fluo3 fluorescence emission using a self-ratio equation as described previously (Tárnok and Ulrich 2001; Martins et al. 2005) assuming a dissociation constant (Kd) of 450 nM for Fluo3-Ca^{2+} binding. Images were collected every second at 20–22 °C. Variations in $[Ca^{2+}]_i$ were calculated for cell populations containing at least 10 cells each. Data were calculated as a percentage of F/F_0 with F and F_0 being Fluo-3 fluorescence emissions of stimulated and unstimulated cells, respectively.

Cell viability

Undifferentiated and differentiated P19 cells were removed from cell culture flasks or dishes by trypsinization, followed by inactivation of trypsin by the addition of medium with 10% FBS. The number of cells was determined using a Neubauer chamber. Cell viability was detected by staining for 1 min with 0.004% Trypan Blue and reported as the ratio between total cells and Trypan Blue-stained dead cells.

Oxygen uptake measurements

Oxygen consumption by 10^6 P19 or E14Tg2A cells suspended in Krebs medium at a controlled temperature (37 °C) was measured using a computer-interfaced Clark-type oxygen electrode (Hansatech Instruments) in a glass cuvette equipped with a magnetic stirrer. Oligomycin (2 μM) and CCCP (1 μM) were added in order to estimate respiratory rates (Fraichard et al. 1995). Oxygen consumption of BLC57 mice whole brain homogenates at 14 days embryonic development, newborns (1^{st} day) and adults was measured using a high resolution Oroboros® oxygraph. The tissues were processed in small pieces of 6 mg weight and ressuspended in 1 mL PBS containing 10 mM glucose in the absence or presence of 2 μM oligomycin and 1 μM CCCP.

Glucose consumption and lactate release

Cell culture supernatants of a 48 h culture of undifferentiated and differentiated P19 cells were used to quantify glucose consumption and lactate release using a commercial glucose

monitor (Accu-Chek, Roche, Brazil) and lactate detection kit (Bioclin, Belo Horizonte, Brazil). Amounts of glucose consumption and lactate production were normalized to the number of cells.

Citrate synthase activity

The conversion of oxaloacetate and acetyl-CoA into citrate and SH-CoA is catalyzed by citrate synthase. For quantification of citrate production, 10^6 trypsinized undifferentiated or differentiated P19 cells were resuspended in 50 mM Tris–HCl, pH 8.0 containing 0.1% Triton X-100, 250 mM oxaloacetate, 50 mM acetyl CoA, 100 mM dithionitrobenzoic acid (DTNB). Following 5 min of incubation at 37 °C and continuing stirring, the absorbance of the reaction product, thionitrobenzoic acid (TNB) was determined at 412 nm in a spectrophotometer (Carry 50, Varian, Australia) (Shepherd and Garland 1966).

Mitochondrial membrane potential determination

P19 cells were permeabilized with 0.008% digitonin in HEPES buffer, pH 7.4, containing 150 mM KCl, 5 mM $MgCl_2$, 100 μM EGTA, 2 mM potassium phosphate and 0.1 mg/mL bovine serum albumin. The membrane potential was continuously monitored using safranin O (5 μM) as fluorescent probe at excitation and emission wavelengths of 495 and 586 nm, respectively, in a fluorimeter (F4500, Hitachi, Japan) (Nicholls and Ferguson 2002). Fluorescence calibration curves were obtained using a gradient of known K^+ concentrations (Nicholls and Ferguson 2002). The membrane potential value obtained for each K^+ concentration was determined using the Nernst equation, assuming intramitochondrial $[K^+]$ to be 150 mM, and plotted against measured fluorescence values to generate a calibration curve for undifferentiated and differentiated P19 cells.

Statistical analysis Data were analyzed with GraphPad Prism or Origin software. Unpaired two-tailed *t*-test comparisons were made to compare different experimental conditions with control measurements. Data shown as traces are representative of at least three independent experiments yielding similar results. Calculated mean values ± SEM refer to experiments carried out at least in triplicate.

Results

P19 EC and E14TG2A ES cells differentiate into functional neurons

Two cell lines were adopted here as in vitro models of neuronal differentiation: P19, an EC line, and E14TG2A, an ES line. P19 cells were differentiated into neurons in the presence of RA, and glial cells were eliminated from differentiating neuron cultures by addition of cytosine-arabinoside. Immunocytochemical reactions were employed using antibodies against proteins specific for undifferentiated cells and differentiated neurons. Undifferentiated EC expressed the stem cell marker SSEA-1, but not βIII tubulin. On the other hand, almost all differentiated P19 cells were positive for βIII tubulin immunostaining, with few cells expressing SSEA-1, confirming efficient neuronal differentiation (data not shown) as determined in previous studies of our laboratory (Resende et al. 2007; 2008a,b). Differentiation of P19 cells into neurons is also accompanied by functional expression of neurotransmitter receptors triggering calcium fluxes into the cells (Resende et al. 2008a, b). Neuronal-differentiated P19 cells responded in calcium-imaging experiments to stimulation with carbamoylcholine, ATP, nicotine, and glutamate, in agreement with previous studies (Ulrich and Majumder 2006; Resende et al. 2008a, b). Thus, P19 cells are an adequate model to study mechanisms of neurogenesis in vitro under our experimental conditions.

However, some concerns may arise regarding the significance of data collected with the P19 cell line due to its cancer cell origin. Therefore, we used a second model, the E14Tg2A mouse embryonic cell line, for our experiments. As well as in EC cells neuronal differentiation was induced in this line and immunocytochemical reactions were employed to confirm the differentiation efficiency (Fig. 1). Functional neurotransmitter receptor and voltage-operated ion channel expression were also analyzed (Fig. 2). Overall, both cell lines presented clear characteristics of neuronal differentiation in vitro. Differentiated cells responded with transient elevations of intracellular free calcium concentration $[Ca^{2+}]_i$ to stimulation of the neurotransmitters ATP and carbamoylcholine (CCh) as well as to membrane depolarization by KCl.

Neuronal differentiation of P19 and E14TG2A cells involves a shift from oxidative to fermentative glucose metabolism

The participation of fermentation and aerobic oxidation of glucose in energy production during neuronal differentiation was studied by measuring oxygen consumption of undifferentiated and differentiated (day 8) P19 cells. The rates of oxygen consumption associated with oxidative phosphorylation can be estimated in intact cells through treatment with oligomycin, which inhibits the mitochondrial F_1F_O ATP synthase, while maximal respiratory rates are achieved by treating cells with the proton ionophore CCCP, which disrupts the inner mitochondrial membrane potential, uncoupling respiration from oxidative phosphorylation (Nicholls and Ferguson 2002). See a representative trace

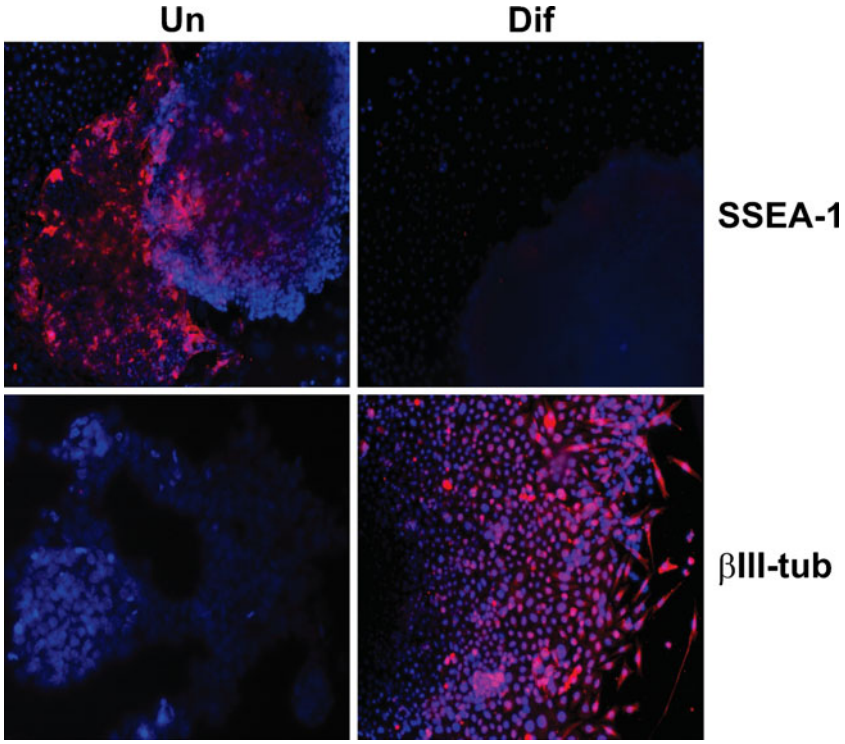

Fig. 1 Neuronal differentiation of E14Tg2A cells. Undifferentiated and differentiated E14Tg2A cells were grown and differentiated in 24 well plate slides. Cells were fixed with 4% para-formaldehyde in PBS, washed and then submitted to immunostaining as described in Experimental Procedures. Most differentiated Tg2a cells expressed βIII tubulin, while a few cells were SSEA-1 positive. The opposite was observed in undifferentiated cells

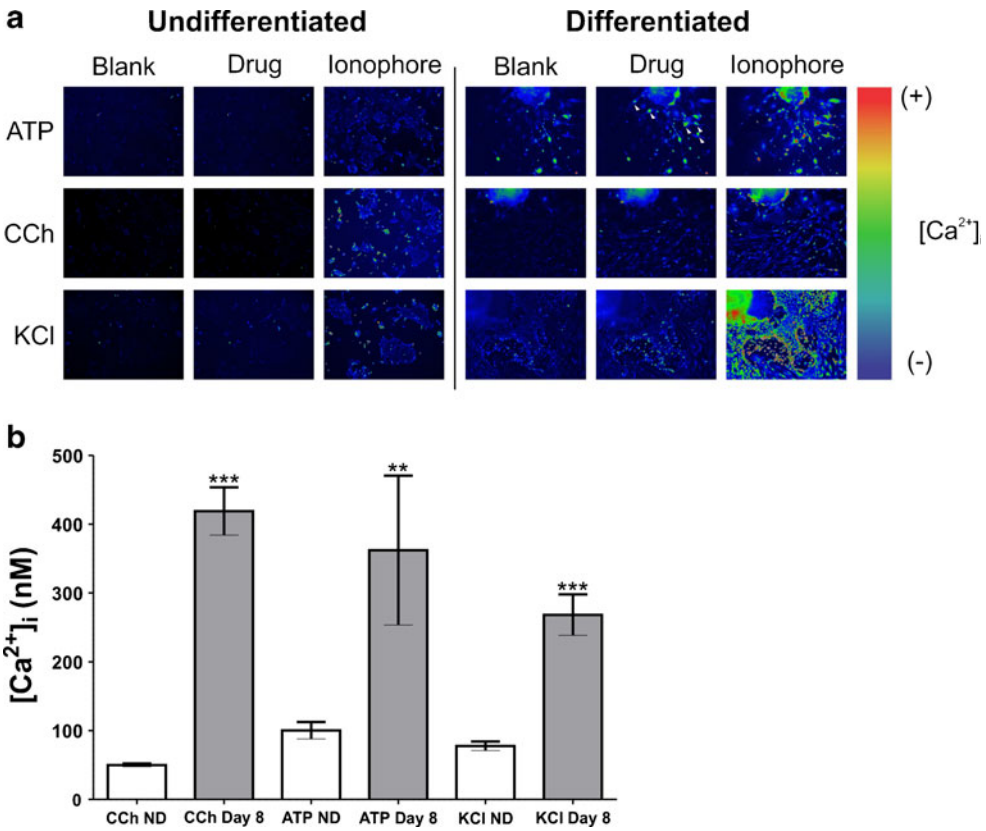

Fig. 2 Expression of functional neurotransmitter receptors and voltage-operated ion channels in neuronal-differentiated E14Tg2A cells. E14Tg2A cells were loaded with the Ca^{2+}–sensitive probe Fluo3-AM, stimulated by neurotransmitters (1 mM ATP or carbamoylcholine, CCh) or a depolarizing agent (100 mM KCl). Subsequent transients in $[Ca^{2+}]_i$ were recorded. Responses were more pronounced in differentiated cells when compared to embryonic cells. A Ca^{2+} ionophore was employed for verification of the live cell population and measurement of the maximal $[Ca^{2+}]_i$ response

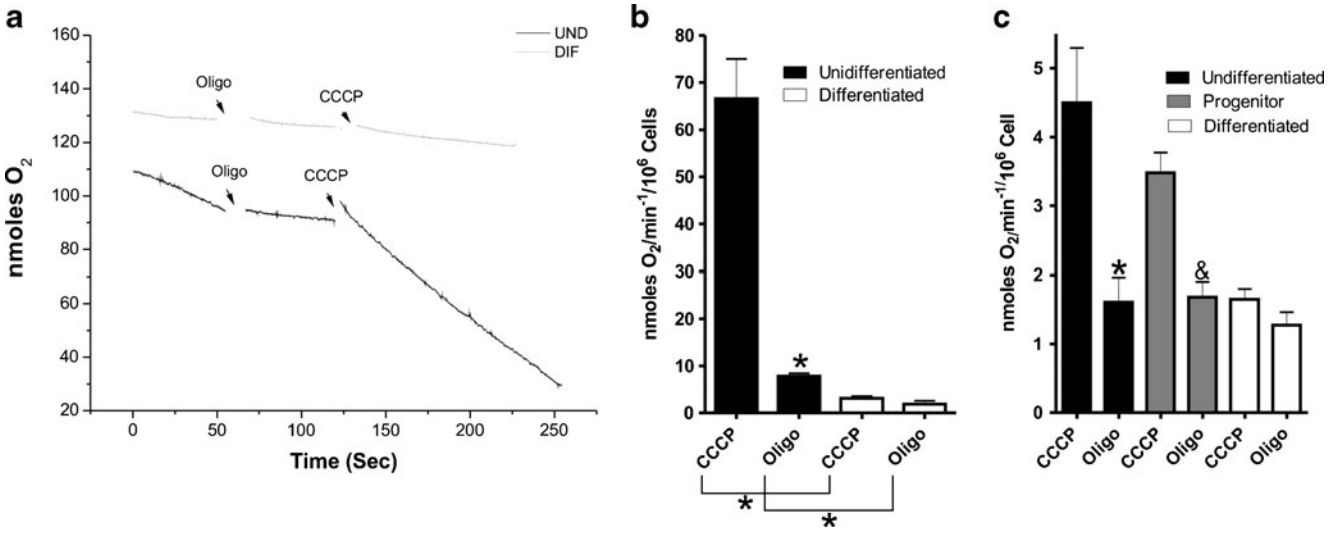

Fig. 3 O_2 consumption by P19 and E14Tg2a cells. Cells were incubated with Krebs buffer and O_2 consumption was estimated as described in Experimental Procedures. **a** Representative traces of respiratory activity in undifferentiated and differentiated E14Tg2a cells; **b** O_2 consumption of E14Tg2A cells *, $p<0.005$ state 3 versus state 4; **c** O_2 consumption of undifferentiated, progenitor stage (day 4) and neuronal-differentiated P19 cells *, $p<0.005$ state 3 versus state 4

in Fig. 3a. In preliminary experiments, both drugs were titrated into cell samples to uncover the ideal concentrations for use in intact cells.

Undifferentiated P19 cells presented a clear difference in maximal respiratory rates promoted by CCCP addition and rates in the presence of oligomycin (Fig. 3b), indicating that their mitochondria are coupled and display a high capacity for oxidative phosphorylation. On the other hand, as these cells developed into progenitor and differentiated cells, maximal respiratory rates decreased and the difference in rates between oligomycin and CCCP-treated cells disappeared, indicating that these cells lost oxidative phosphorylation capacity during the differentiation process. The observed metabolic changes did not result from decreased viability, as shown by the absence of Trypan Blue inclusion in the cell types at all times during differentiation (Supplementary Fig. 1). We also questioned if cytosine arabinoside, an inhibitor of glial proliferation used in the differentiation protocol, could interfere with glucose metabolism under our conditions, and performed experiments with cells differentiated in the absence of this compound, rendering identical results (Supplementary Fig. 2). The decrease in maximal respiratory capacity during differentiation associated with more similar respiratory rates in the presence of CCCP and oligomycin was also observed in E14Tg2A ES cells (Fig. 3c). This suggests that lower respiratory capacity and uncoupling of respiration from oxidative phosphorylation are a general phenomenon occurring during neuronal differentiation.

While changes in maximal respiratory capacity suggest the presence of less functional mitochondrial respiratory chains in differentiated cells, usually associated with lower mitochondrial biogenesis, the loss of differences between maximal and oligomycin-inhibited respiration suggest mitochondrial uncoupling, usually promoted by changes in inner membrane integrity and impermeability to protons. In order to verify if mitochondrial content was indeed smaller in differentiated cells using a second technical approach, we measured citrate synthase activity, a commonly-used marker of mitochondrial biogenesis (Civitarese et al. 2007). Consistently with our prior results, we found that citrate synthase activity was significantly reduced in differentiated cells (Fig. 4a).

We also measured mitochondrial inner membrane potentials in the absence of oxidative phosphorylation in order to uncover changes in mitochondrial coupling. To do so, we permeabilized cells with digitonin, which interacts with cholesterol, therefore preserving mitochondrial intactness (Fiskum et al. 1980). We then used safranine O fluorescence traces calibrated by extramitochondrial K^+ additions to quantify membrane potentials (Kowaltowski et al. 2002). We found that mitochondria within differentiated neurons presented significantly lower inner membrane potentials (Fig. 4b), a result compatible with the indications of mitochondrial uncoupling provided by respiratory quantifications in Fig. 3. Despite their lower mitochondrial activity, differentiated cells presented much higher glucose consumption rates (Fig. 4c), a finding compatible with the high energy demand of this tissue. The high glucose consumption in the absence of elevated respiratory activity in these cells suggests enhanced glycolysis. Indeed, we found that differentiated cells produce ~200 times more lactate than undifferentiated cells (Fig. 4d). Altogether, these results demonstrate that differentiating neurons undergo a shift from oxidative to fermentative glucose metabolism, associated with a decrease in mitochondrial activity and mitochondrial uncoupling.

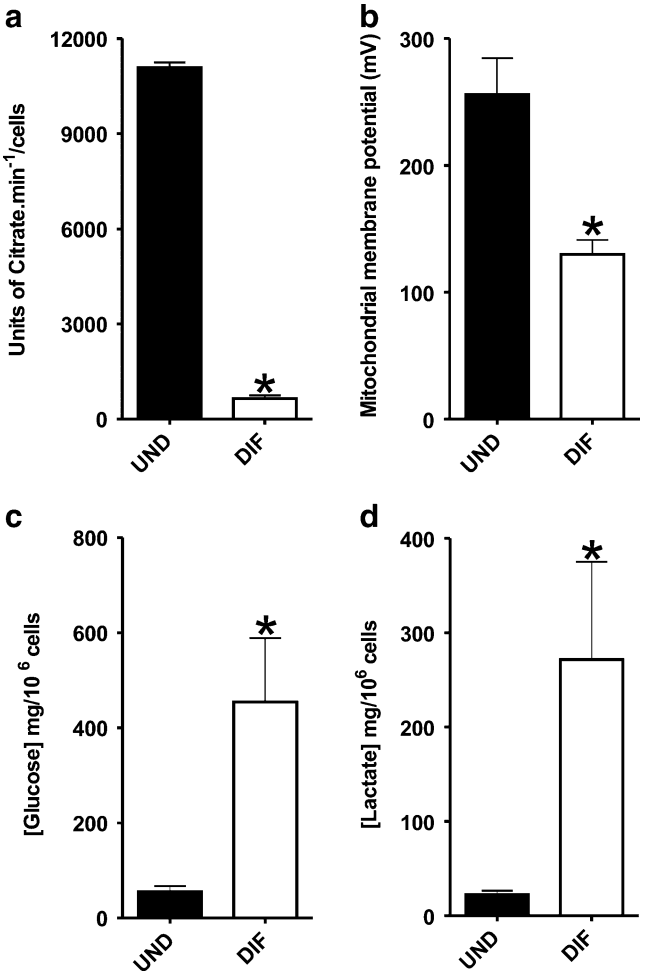

Fig. 4 P19 cell metabolism. **a** Permeabilized P19 cells were incubated in 150 mM KCl, 5 mM Hepes, 1 mg/mL BSA, 100 μM EGTA, 5 mM Mg^{2+} and 1 mM ATP. **a** Permeabilized P19 cells were incubated in Tris–HCl and citrate release was accompanied to measure citrate synthase activity; *$p<0.005$; **b** Mitochondrial membrane potentials were measured through fluorescence changes of 5 μM safranin O as described in Materials and Methods; *, $p<0.05$ versus control; **c** and **d** The culture medium of P19 cells was collected and glucose consumption and lactate released were monitored as described in Experimental Procedures. *$p<$ 0.005. UND = Undifferentiated cells; DIF = Neuronal-differentiated cells

Oxidative phosphorylation is not essential for neuronal differentiation

In view of the changes we observed in glucose use from undifferentiated to differentiated cells, and evidence that mitochondrial respiration is unnecessary to maintain neuronal viability (Budd and Nicholls 1996; Nicholls and Budd 1998); Castilho et al. 1998), we questioned if oxidative phosphorylation is necessary for the process of neuronal differentiation. We thus induced P19 differentiation with RA in the presence of oligomycin, present in the culture media for 8 days. The experiments were performed in the absence of cytosine arabinoside to uncover the effects of oligomycin on both neuronal and glial differentiation. We found that cells differentiated normally under these conditions, as indicated by changes in morphology (Fig. 5a), expression of βIII tubulin in oligomycin-treated and control cells (Fig. 5b).

Respiratory changes during embryonic development

Our results indicate that cell differentiation is accompanied by a change from respiration towards fermentation of glucose. However, these results may reflect simplified conditions of in vitro neurogenesis. We thus sought experimental evidence that a similar process occurs in vivo. We measured

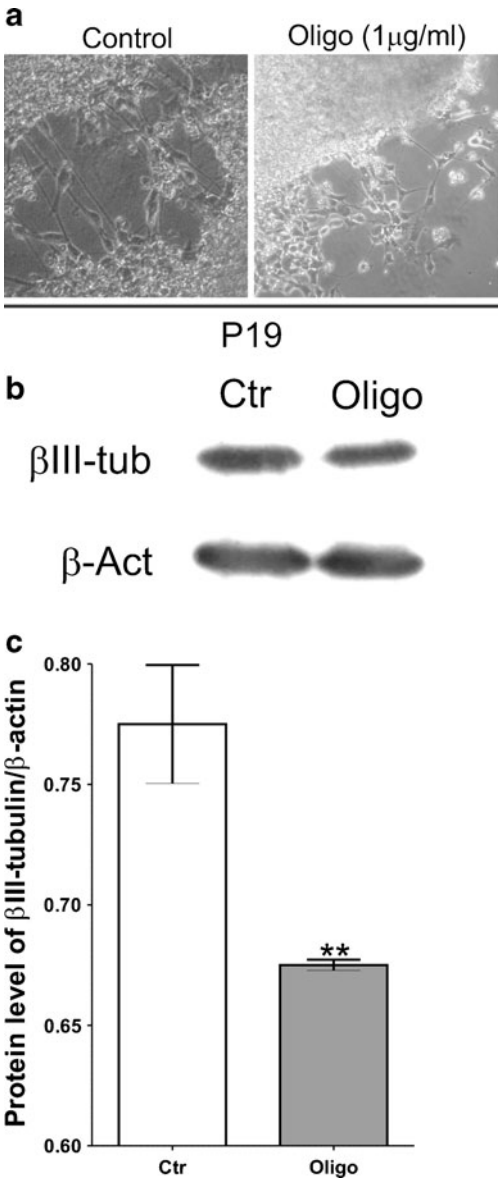

Fig. 5 Differentiation of P19 cells in the presence of oligomycin. P19 cells were cultured with 1 μM oligomycin during differentiation. The drug was readministered with medium changes, performed every 48 h. **a** Differentiated P19 cell; **b** Western-blot analysis of βIII tubulin expression in control cells (DMSO) and cells treated with oligomycin compared to β actin (β Act) expression as internal control

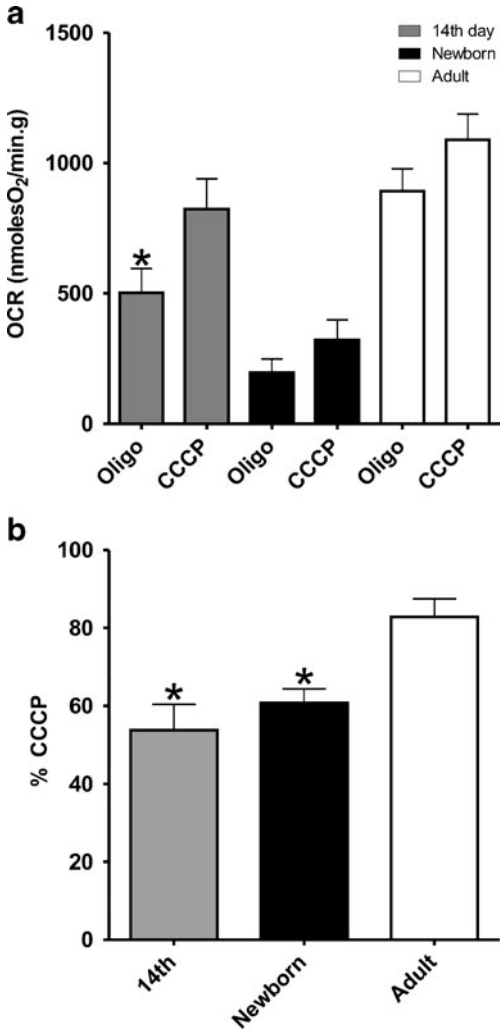

Fig. 6 O_2 consumption during neuronal development. Brains of BLC57 mice were minced, resuspended in PBS supplemented with 10 mM glucose and O_2 consumption was determined. ATP-linked and maximal respiration were measured in the presence of 2 μM oligomycin and 2 μM CCCP, respectively. **a** Respiration of embryonal, newborn and adult brain tissues; **b** Respiratory ratios of oligomycin-inhibited and CCCP-stimulated tissues

oligomycin-inhibited and CCCP-stimulated respiration in homogenates from BLC57-strain mice brains from the 14th day of embryonal development (E14), newborns (1st day) and adults (Fig. 6). Similarly to our in vitro studies, we found that the difference between maximal, CCCP stimulated, and oligomycin inhibited respiration decreased with development (Fig. 6a). In fact, in adult animals, almost the totality of respiratory activity was oligomycin-insensitive, indicating that it was not coupled to ATP synthesis (Fig. 6b).

Discussion

P19 EC and E14Tg2A ES cells were employed as in vitro models to study changes in glucose metabolism during neurogenesis. Both P19 and E14Tg2A cells are adequate models for neuronal differentiation, revealing phenotypic transitions characteristic for neuroectodermal development. Undifferentiated P19 cells express the pluripotency marker SSEA-1, while differentiated cells express neuron-specific βIII tubulin, functional neurotransmitter receptors and voltage-gated ion channels (Ulrich and Majumder 2006; Resende et al. 2008a; Martins et al. 2005; Resende et al. 2007). E14Tg2A cells, used as a second model to confirm metabolic changes observed in P19, also revealed phenotypic changes from pluripotent stem cells toward differentiated neurons. Neuronal-differentiated E14Tg2A cells also expressed βIII tubulin and were responsive to neurotransmitter receptor agonists nicotine, carbamoilcholine or ATP, as verified in calcium-imaging experiments shown in Fig. 2.

During the course of neuronal differentiation, oxygen consumption of both P19 and Tg2A cells decreased and the remaining respiration became increasingly uncoupled from oxidative phosphorylation. Oxygen consumption was decreased in neural-progenitor cells at an intermediate state of differentiation when compared to undifferentiated cells. It was, however, higher than in differentiated cells, indicating that the decline in oxygen production and rise in uncoupling was directly proportional to the advancement of neurogenesis.

In agreement, glucose metabolism was higher in differentiated cells compared to undifferentiated control cells. Moreover, lactate production was strongly enhanced in neuronal-differentiated cells. Previous studies suggested that glial cells primarily consumed glucose and produced lactate, then used by neurons as a substrate to produce ATP via oxidative metabolism (Pellerin and Magistretti 1994). Our present results contrast with these, since we found that oxidative phosphorylation did not play a major role in energy production in differentiated neurons when compared to undifferentiated cells.

The loss of mitochondrial activity and concurrent uncoupling was confirmed through measurements of citrate synthase activity and mitochondrial membrane potential determinations. Following induction to differentiation, P19 cells have decreased mitochondrial membrane potentials and citrate synthase activity was strongly decreased. These results corroborate our findings regarding O_2 consumption (Fig. 3). Furthermore, oxidative phosphorylation was not essential for neurogenesis, since cells underwent differentiation into neuronal phenotypes in the presence of the ATP synthase inhibitor oligomycin. Our hypothesis is that the brain conducts glycolysis in order to provide ATP at rates fast enough for the demand of active transport rising from neurotransmission.

Our in vitro results are supported by experiments measuring O_2 consumption in different stages of neuronal development using cell extracts from fetal (E14), newborn and adult brains. On day 14 of embryonic development

(E14), the nervous system is predominantly composed by neural progenitor cells, while in the newborn brain neurogenesis is almost complete, although cerebellar development occurs in the post-natal period (Wang and Zoghbi 2001). Adult brains are composed by mature neurons and glial cells. As verified during in vitro neurogenesis, in vivo brain development was also accompanied by uncoupling and a decrease in respiratory activity.

Overall, our results measuring respiratory activity coupled or not to oxidative phosphorylation in two in vitro models as well as in vivo indicate that neural differentiation is accompanied by a shift from respiratory to fermentative metabolism of glucose. The signaling events which induce this shift in energy metabolism have not yet been identified, but the end result is a decrease in mitochondrial activity and uncoupling, associated with increases in lactate production. Interestingly, the brain is a highly demanding tissue from an energetic standpoint, and was always believed to rely mostly on oxidative phosphorylation. Although the reasons for a shift to glycolysis are as of yet unclear, we hypothesize it could be advantageous to support ATP demands through fermentation due to its fast response under conditions of high ATP turnover such as in the stimulated brain. Altogether, our results provide a new insight into the metabolic characteristics of adult and differentiating brain tissue.

Acknowledgments This work was supported by grants awarded by FAPESP (Fundação de Amparo à Pesquisa do Estado de São Paulo) and CNPq (Conselho Nacional de Desenvolvimento Científico e Tecnológico), Brazil (to H.U. and A.J.K.). M.F.'s postdoctoral research was funded by Coordenação de Aperfeiçoamento de Pessoal de Nível Superior (CAPES-PNPD). I.C.M.'s and A.A.N.'s Ph.D. thesis research projects are currently supported by FAPESP.

References

Bain G, Ray WJ, Yao M, Gottlieb DI (1994) Bioessays 16:343–348
Bain G, Kitchens D, Yao M, Huettner JE, Gottlieb DI (1995) Dev Biol 168:342–357
Bernstein BW, Bamburg JR (2003) J Neurosci 23:1–6
Bittar PG, Charnay Y, Pellerin L, Bouras C, Magistretti PJ (1996) J Cereb Blood Flow Metab 16:1079–1089
Bolaños JP, García-Nogales P, Vega-Agapito V, Delgado-Esteban M, Cidad P, Almeida A (2004) J Neurochem 63:910–916
Budd SL, Nicholls DG (1996) J Neurochem 67:2282–2291
Castilho RF, Hansson O, Ward MW, Budd SL, Nicholls DG (1998) J Neurosci 18:10277–10286
Civitarese AE, Carling S, Heilbronn LK, Hulver MH, Ukropcova B, Deutsch WA, Smith SR, Ravussin E, CALERIE Pennington Team (2007) PLoS Med 4:e76
Cox DWG, Bachelard HS (1982) Brain Res 239:527–534
Dinsmore J (1996) Cell Transpl 5:131–141
Fiskum G, Craig SW, Decker GL, Lehninger AL (1980) Proc Natl Acad Sci USA 77:3430–3434
Fraichard A, Chassande O, Bilbaut G, Dehay C, Savatier P, Samarut J (1995) J Cell Sci 108:3181–3188
Hertz L (2007) J Cereb Blood Flow Metab 27:219–249
Hooper M, Hardy K, Handyside A, Hunter S, Monk M (1987) Nature 326:292–295
Hyder F, Patel AB, Gjedde A, Rothman DL, Behar KL, Shulman RG (2006) J Cereb Blood Flow Metab 26:865–877
Jones-Villeneuve EM, McBurney MW, Rogers KA, Kalnins VI (1982) J Cell Biol 94:253–262
Kasischke KA, Vishwasrao HD, Fisher PJ, Zipfel WR, Webb WW (2004) Science 305:99–103
Keller G (2005) Genes Dev 19:1129–1155
Kowaltowski AJ, Cosso RG, Campos CB, Fiskum G (2002) J Biol Chem 277:42802–42807
Magistretti PJ (2006) J Exp Biol 209(Pt 12):2304–2311
Martins AH, Resende RR, Majumder P, Faria M, Casarini DE, Tárnok A, Colli W, Pesquero JB, Ulrich H (2005) J Biol Chem 280:19576–19586
Mcllwain H, Bachelard HS (1985) In: Biochemistry and the central nervous system. Churchilll Livinstone, Edinburg. pp 54–83
Nicholls DG, Budd SL (1998) Biochim Biophys Acta 1366:97–112
Nicholls DG, Ferguson SJ (2002) In: Bioenergetics 3, Academic, London
Pauwels PJ, Opperdoes FR, Trouet A (1985) J Neurochem 44:143–148
Pellerin L, Magistretti PJ (1994) Proc Natl Acad Sci USA 91:10625–10629
Rehman J (2010) J Mol Med 88:981–986
Resende RR, Majumder P, Gomes KN, Britto LR, Ulrich H (2007) Neurosci 146:1169–1181
Resende RR, Alves AS, Britto LR, Ulrich H (2008a) Exp Cell Res 314:1429–1443
Resende RR, Britto LR, Ulrich H (2008b) Int J Dev Neurosci 26:763–777
Shepherd D, Garland PB (1966) Biochem Biophys Res Commun 22:89–93
Sibson NR, Dhankhar A, Mason GF, Rothman DL, Behar KL, Shulman RG (1998) Proc Natl Acad Sci USA 95:316–321
Soprano DR, Teets BW, Soprano KJ (2007) Vitam Horm 75:69–95
Tárnok A, Ulrich H (2001) Cytometry 43:175–181
Tsacopoulos M, Magistretti PJ (1996) J Neurosci 16:877–885
Ulrich H, Majumder P (2006) Cell Prolif 39:281–300
Véga C, Poitry-Yamate CL, Jirounek P, Tsacopoulos M, Coles JA (1998) J Neurochem 71:330–337
Wada H, Okada Y, Uzuo H, Nakamura H (1998) Brain Res 788:144–150
Wang VY, Zoghbi HY (2001) Nat Rev Neurosci 2:484–491
Warburg O (1956) Science 124:269–270
Yamane K, Yokono K, Okada Yasuhiro O (2000) J Neurosci Methods 103:163–171